Development and Electric Grid Applications of a Magnetometer Network

Komal S Shetye, *Senior Member, IEEE,* Ramyaa Rathna Kumar, Cecilia Klauber, *Student Member, IEEE,* Zeyu Mao, *Student Member, IEEE,* Thomas J Overbye, *Fellow, IEEE,* Jennnifer Gannon, *Member, IEEE,* and Michael Henderson

***Abstract*—Monitoring the elements associated with geomagnetic disturbances (GMDs), such as the earth's magnetic field, can help mitigate their negative impacts on the power grid. While there are existing magnetometers monitoring this in certain locations, they are currently sparse and have several gaps in coverage such as the southern US region. This paper describes the recently developed network of six magnetometers in the US state of Texas. Aspects such as the site selection, physical description of a magnetometer station, and data communication are described. Data quality is tested using correlation analysis among these magnetometers and pre-existing magnetic observatories. A real-time magnetic field data streaming and visualization setup is developed, with provisions to make the data available to researchers and industry.**

***Index Terms*—geomagnetic disturbances, geomagnetically induced currents, GMD, GIC, magnetic field, measurements**

I. Introduction

Geomagnetic disturbances (GMDs), which are caused by solar coronal mass ejections (CMEs), are known to create large disruptions in the magnetic field surrounding the earth. It is well known by now that power system grid operations can be largely influenced by such events [1]. Interaction of a changing magnetic field with the earth conductivity induces an electric field at the surface, which in turn causes quasi dc currents, known as geomagnetically induced currents (GICs) to flow in long conductors with earth connections, such as the power grid [2]. These have adverse effects on major power system components, especially transformers [3], [4].

The North American Electric Reliability Corporation (NERC) highlights in their report on the assessment of GMD effects, two primary risks associated with GMD events: 1) the potential for damage to high voltage transformers, and 2) the potential for voltage collapse due to GMD-induced reactive power losses [5], [6]. To elaborate, GICs can cause overheating and damage to the transformers, with high circulating currents leading to the saturation of transformers [7]. The currents can also cause relays, capacitive components such as Static Var Compensators (SVCs), and other protection devices to trip, contributing to grid instability; this effect is compounded by the fact that transformers already absorb extra reactive power due to GICs [8]. In view of all these potentially catastrophic effects that GMDs can have on the electric power grid, it is important to monitor GMD event drivers, a key one being the local magnetic field. This data can benefit both the power industry and research communities. Increased monitoring can aid in improved power system planning and operations with respect to responding to GMDs [9].

Magnetometers are devices which measure the earth's magnetic field. This data can be transmitted across the internet to a central server for recording in a database. Currently, there are a number of magnetometers measuring the earth's magnetic field in different locations around the world. Some of the major networks these belong to include the following:

1) US Geological Survey (USGS) observatories [10].
2) INTERMAGNET i.e. the International Real-Time Magnetic Observatory Network which aggregates data from qualifying national observatory programs according to certain standards [11]. Magnetic observatories typically produce long-term, continuous, high quality records of data. This is achieved by making regular absolute measurements to determine baselines for the continuous recordings. The network includes 57 institutes from 40 countries, with data from 120 observatories [12].
3) SuperMAG, a worldwide collaboration of organizations and national agencies that currently operate more than 300 ground based magnetometers [13], including variometers, which are not meant to record observatory quality data. The key differences between variometers and observatories arise from, 1) the limited control over the long-term absolute level of the field with a variometer, owing to factors such as temperature dependence, and 2) the orientation and long-term stability of variometers not being as tightly controlled as the observatory instruments [14]. However, both variometers and observatory instruments are useful in space weather and related fields. In GMD applications, where the change in the magnetic field is more important than the absolute value, variometers can be a technically sound and cost effective way of monitoring the field. SuperMAG, also provides a higher spatial density of instruments compared to the observatory network.
4) IMAGE network which consists of 41 magnetometer stations maintained by eight institutes in Northern Europe

The work described in this paper was supported by funds from Texas A&M University and the State of Texas Governor's University Research Initiative (GURI) grant program.

K.S. Shetye, R.R. Kumar, C. Klauber, Z. Mao, and T.J. Overbye are with the Department of Electrical and Computer Engineering, Texas A&M University, College Station, TX, USA; (email: {shetye, ramyaarathnamanjula, cklauber, zeyumao2, overbye}@tamu.edu).

J. Gannon and M. Henderson are with Computational Physics, Inc., Boulder, CO, USA; (email: gannon@cpi.com, mphend@gicmagnetics.com).

in high latitude regions [15].

As the USGS Geomagnetism Program monitors the earth's magnetic field at 14 locations across the country, with less than half of them located in the continental US [16], measurement sparsity is a concern for GMD event recreation and other research. For example, in [17] the closest magnetometers to the transformer neutral GIC measurements of interest were over 800 miles away and approximations using interpolation were made to perform model validation. Filling in some of these gaps by installing magnetometers can improve observability and provide any hitherto missing data on local field variations.

Installing closely spaced magnetometers can enhance existing research initiatives as well as propel new research on the benefits and usage of data from such denser magnetometer arrays, which are currently found mostly in very high latitude regions such as Alaska and Finland. Higher frequency magnetic field variations have shorter correlation lengths. Hence, we may be missing some high frequency information from GMD storms by considering data from magnetometers which are very far apart. In addition, observations of local electric field enhancements (also referred to as electric field hotspots) which are now very commonly used in GMD assessments, were made possible only by arrays of closely spaced magnetometers. The exact cause of this hotspot phenomenon is not known, except that it originates in the ionospheric current system. A dense array at a lower latitude could help determine whether hotspots can occur in this region and provide more insight on what causes them.

Increased availability of magnetometer data can supplement GMD research such as model validation and enable situational awareness and real-time control and monitoring applications. Earth conductivity models are particularly important in GIC analysis but are known to have uncertainty. It is well known in the geophysics and power systems communities that there is significant uncertainty in the existing conductivity models of Texas and nearby areas [18]. Such magnetic field measurements coupled with electric field measurements or with measured transformer GICs can help validate and improve earth conductivity models, leading to better assessments of GMD effects, and more accurate real-time GIC calculations.

Regarding monitoring and control, gathering, analyzing, and visualizing large amounts of magnetometer data can help operators assess the impacts of GMDs on their systems in real-time and act quickly and effectively to mitigate GIC impacts. On the planning time scale, this data could be used to inform the installation of GIC blocking devices and other mitigative plans [19]. The motivation to install magnetometers also lies in the increasing emphasis on GMD monitoring specified by NERC TPL-007 standards [20], as well as in the space weather community [21]. Besides GMDs and beyond the power grid, magnetometer data can be of benefit to the field of seismology and other geophysical interests.

The purpose of this paper is to describe the relevance and process of procuring, visualizing, and analyzing magnetic field data with implications for managing GICs in the power grid. A description of Texas A&M University's (TAMU) newly installed network of magnetometers in the US state of Texas is presented. A key contribution of this paper is the provision of important factors that need to be considered for a real magnetometer setup. The rest of the paper is organized as follows: Section II describes the magnetometer setup including site selection, physical description of the equipment, and data communication. Section III details the correlation analysis of the data, while Section IV highlights visualizations of the magnetometer data. Several insights are discussed based on the analysis results and visualizations. Section V summarizes the paper, with future work directions.

II. Magnetometer Network

The Texas A&M University Magnetometer Network (TAMUMN) captures the magnetic field at locations shown in Fig 1. The installations consist of a magnetic field sensor, data acquisition and transmission unit, and a solar power system. These data are recorded at a cadence of 1 Hz and transmitted in real time (latency < 10 ms) to a data center (server) at TAMU, for the purposes of display, access, and archiving. The setup of this network and its key components are discussed below.

A. Site Selection

This is one of the most important steps in the overall process of installing a single or a network of magnetometers. Due to the nature of the measurements and the device, the site needs to satisfy certain key requirements, which limit the number of potential locations. The site should be magnetically quiet, i.e. no ferrous metals, current-carrying wires, fences, buildings, roads (i.e. cars) nearby. This includes power lines and underground pipelines, and hence this process requires careful investigation and survey of any potential site. Since utilities have been looking into installing magnetometers to supplement their transformer GIC monitors, substations may appear to be potential sites. However, there are significant complications in installing a magnetometer near a substation due to the presence of the grounding mat and high level of possible magnetic noise.

Determining the exact required minimum distance between a magnetometer and magnetic/ferrous objects is a difficult problem. However, there are certain ballpark distances known that can be used to inform site selection. For instance, the measurement accuracy required at magnetometer stations is 5 nT or better. A useful rule-of-thumb is that the distance from a ferrous object at which the influence falls below 1 nT is about 20 times the maximum dimension of the object [22]. With these estimates, a car passing by or a road should be at least 60 m away from the magnetometer.

In selecting the sites for the six magnetometers of the TAMUMN, the idea was to distribute them across the state of Texas for maximum coverage. Another consideration was to locate them close to at least some existing GIC monitors to enable model validation research since it needs very good measurements or estimates of the magnetic field at the monitored transformer(s). Good correlations of magnetic fields become difficult at distances above 200 miles (322 km) [18]. However, this number is also subject to various model uncertainties. Determining how close they need to be is one of the goals of the research for which this data is being collected. Considering

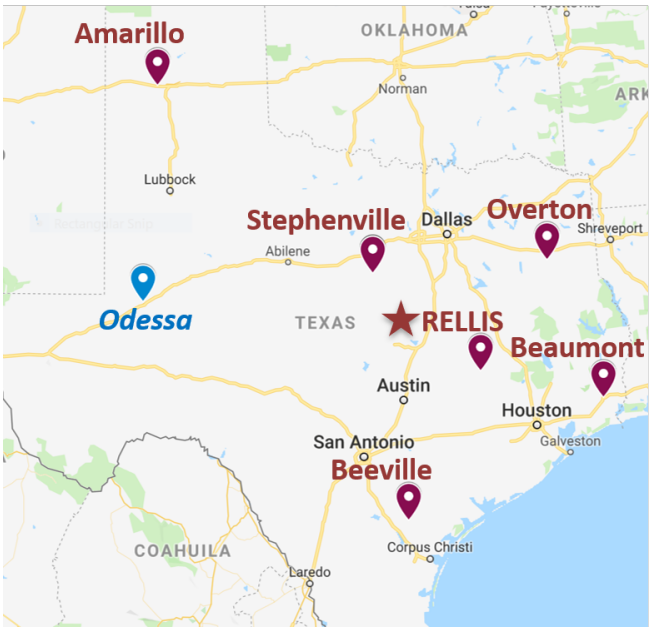

Fig. 1. Magnetometer Network Locations: Amarillo (AMR), Beaumont (BMT), Beeville (BVL), Overton (OVR), RELLIS (RLS), and Stephenville (STP). Odessa (ODS) station in Far West Texas was installed under a prior project; its data will be added to the TAMUMN shortly.

all these factors, the magnetometers were sited at some of the Texas A&M AgriLife campus locations, namely Amarillo (AMR), Beaumont (BMT), Beeville (BVL), Overton (OVR), and Stephenville (STP). The sixth magnetometer is at the RELLIS (RLS) campus in College Station and is also where the server and all the data is hosted. Fig. 1 shows all these magnetometers, with a seventh in far west Texas shown in blue representing an older (currently offline) installation done by the authors from a previous project. Work is ongoing to upgrade this station and add its data to the TAMUMN, to improve estimation of the geoelectric field.

B. Station, Device, and Networking

At each site of the TAMUMN is a (Space Hazard Monitor) SHM^{TM} real-time magnetometer system, which runs autonomously with hardware and software system monitoring to support continuous data transmission [23]. The station is solar powered and operates without human interaction except for routine service or repair. Each station consists of two major parts - the sensor, mounted on aluminum hardware on top of a concrete slab or pillar, and a data acquisition unit (DAQ) located 30 feet away. Magnetometers are sensitive to both electromagnetic noise and to ferrous materials, so the sensor must be located well away from steel objects or places where steel objects may be encountered routinely (for instance, a road or driveway). Because of these issues, site selection can be one of the more difficult steps in placing sensors for GIC hazard analysis. In the placement of sensors for the TAMUMN, iteration on location had to be done in several locations due to unexpected environmental conditions, and local conditions. The 30 ft (~10 m) separation, which can be seen in Fig. 2, between the DAQ and the sensor is also to

Fig. 2. Magnetometer Station

avoid noise from the station's own electronics being introduced into the measurement. The sensor at the heart of the system is a Bartington Mag-13 triaxial fluxgate magnetometer [24]. These are low-noise sensors which produce a set of voltages proportional to the observed magnetic field strength. The SHM^{TM} DAQ produces a 1-Hz 3-component vector sample of the geomagnetic field, time stamped with the UTC second, which is transmitted in real-time to a database archive hosted on a cloud-based virtual machine.

There are two ways to connect the station to the internet; either a point-to-point wireless link to a nearby building with internet access, or a cellular modem. In the first connection scheme, the DAQ is equipped with a wireless ethernet bridge built by Schweitzer Engineering Laboratories (SEL). This is an encrypted, proprietary point-to-point connection. The far end of the wireless link is a second Schweitzer bridge device housed in a building which has existing internet access. An antenna mounted either in a window or outside the building is connected through a feed cable to the modem. While the direct wireless ethernet bridge provides better data continuity, in some locations the lack of local infrastructure makes this impossible. In these cases, a different connection type must be used. The second connection scheme, employed by some sites of the TAMUMN uses a cellular modem inside the DAQ to connect to a commercial cell network and maintain data communications. The station uses an omnidirectional antenna, if possible, to connect to the cell network but can use a high-gain directional antenna if necessary for that location.

C. Data Description

The magnetic field is a vector i.e. it has a magnitude and direction. Two coordinate systems are typically used to represent this vector, i.e. geographic or geomagnetic, with the TAMUMN magnetometers using the former. The x, y, and z axes orthogonal components represent field directions with positive values for geographic northward, eastward, and vertical into the earth, respectively, and negative values for their opposite directions. The magnetic field data is used to calculate the electric field components and hence the GICs.

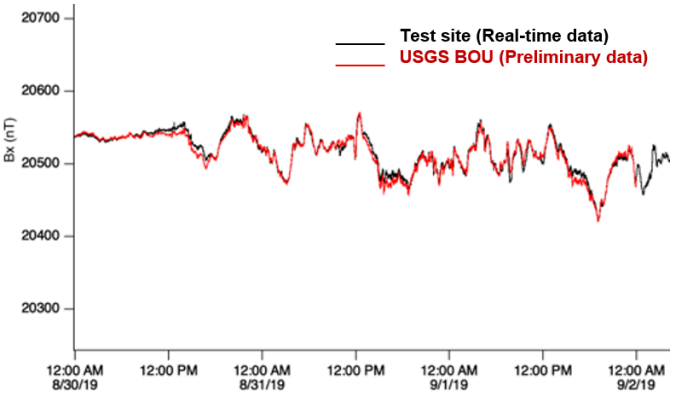

Fig. 3. Magnetometer Data Validation

A virtual machine instance set up at the data center at TAMU consists of data acquisition modules, i.e. a time series database, and receives data from the cloud-based server. Processes are coded to produce text file backups and data access in the standard geomagnetic "International Association of Geomagnetism and Aeronomy" (IAGA) 2002 format [25], provided under Open Source Access, which can be modified by the TAMUMN. IAGA-supported anti-aliasing filters were also used for data downsampling. The data is converted to the JSON format [26], prior to being fed to the database. A time series database is setup to save the real-time data stream efficiently, it also provides a RESTful API for users to query. An online interactive visualization tool is connected to the database and offers a web dashboard for users to browse the data history.

Before the install, the setup designed to be used at all the TAMUMN sites was tested at a remote site. This test installation at Boulder, CO was calibrated with data from the nearby USGS magnetic observatory. Fig. 3 shows these results, for a GMD event that occurred on September 1st, 2019.

This section described the hardware and software setup of the TAMUMN network. This process and its relationship to potential power system monitoring, analysis, and control can be summarized in Fig. 4. This data could be combined with other data sources such as transformer currents from GIC monitors, state estimator output, and other SCADA and/or PMU measurements for improved situational awareness and real-time analyses. The novel GIC estimator proposed in [27], and the GIC-inclusive state estimator described in [28] are examples of such applications.

III. Data Analysis and Examples

This section provides examples of measurements from a GMD event day compared to a normal day, with some initial observations and insights enabled by this network. It also compares the TAMUMN data with that from magnetic observatories as a post-installation data verification step.

A. Correlation Analysis

For this comparison, correlation analysis is used, which is a well-known statistical method. It evaluates the relationship

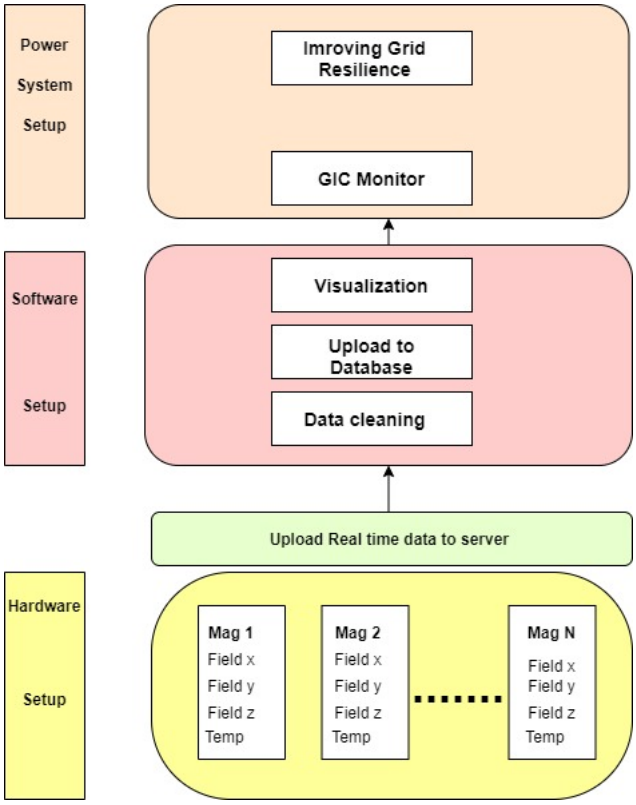

Fig. 4. Flowchart describing software and hardware setup of the magnetometer network for power system applications

Fig. 5. US Magnetometers used in correlation analysis along with TAMUMN. FRN: Fresno, BOU: Boulder, AMR: Amarillo, BSL: Stennis, FRD: Fredericksburg

between two quantitative variables, where results are assigned numerical values between -1 and 1. A high (positive or negative) correlation co-efficient indicates that the variables have a strong relationship. Meanwhile a small value represents a weak correlation and relationship between the variables. Correlation analysis is also applied between the magnetometers of the TAMUMN itself. Fig. 5 shows the locations of the other magnetometers used in this analysis. These are USGS observatories namely, 1) Fresno (FRN), 2) Boulder (BOU), 3) Stennis, formerly known as Bay St. Louis observatory (BSL), and 4) Fredericksbrug (FRD). This is done to further test the validity and quality of the TAMUMN data on a wider scale, compared to existing magnetic observatory-quality data, and to investigate local anomalies, if any.

The analysis is done on the 1-second magnetic field mea-

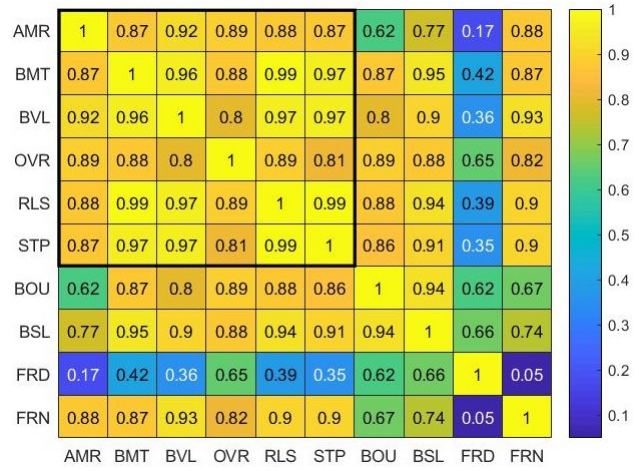

Fig. 6. Correlation between TAMUMN and other US magnetometers on a normal (no GMD event) day; Feb 4, 2020.

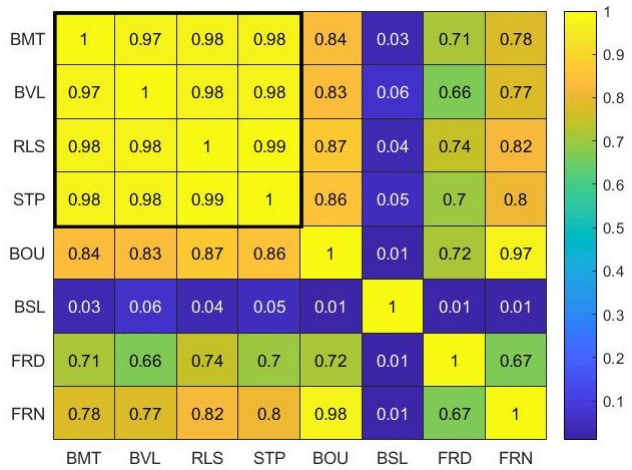

Fig. 7. Correlation between TAMUMN and other US magnetometers on a GMD (G1: minor) event day; Feb 19, 2020.

surements over a 24-hr period using the Pearson's correlation coefficient, which is the covariance of the two variables divided by the product of their standard deviations. Consider X and Y as random variables which indicate the x-component of the magnetic field at two different stations. Since all the three components of magnetic field show similarity in data, the x-component is chosen as it represents the geomagnetic north. This is usually defined as the direction that the local field points in the horizontal plane, either on average or on a "quiet" day when there is little short time scale (< 1 day) variation [29]. The equation for the coefficient is given by,

$$\rho_{XY} = \frac{cov(X,Y)}{\sigma_X \sigma_Y} \tag{1}$$

Here $\sigma_X \sigma_Y$ pertains to the product of standard deviation of the entire data for both the stations selected. The covariance between the stations is divided by this value.

Magnetic field data from other stations is readily available online and downloaded from the INTERMAGNET website [30]. Two days are selected for performing the analysis, 1) February 4th, 2020 when no geomagnetic activity occurred, and 2) February 19th, 2020 when a minor GMD (G1) event was recorded. The correlation results are shown with heat maps in Fig. 6 for the non-event i.e. "normal" day, and in Fig. 7 for the day of the GMD event. Higher correlation is observed among the TAMUMN magnetometers as outlined by the black square in Fig. 6. All the TAMUMN stations are found to be largely correlated (> 0.8) with each other on both a quiet day and a day with minor geomagnetic activity. They are also well correlated with most of the other stations, with some interesting exceptions.

In Fig. 6, FRD is poorly correlated with all other stations on the "normal" day, whereas on the G1 event day, the BSL station shows a very weak correlation with the other stations, and FRD fares better. The BSL station is much closer geographically and also in magnetic latitude to the TAMUMN than FRD is, so it is likely that the magnetic variations caused by the event were more spatially spread out compared to the variations on a normal day. This hypothesis stems from the fact that GMD events typically cover a wide-area, such as on the continental scale. Conversely, the normal day magnetic variations may be more driven by local factors which are exacerbated in the absence of such a wide-area event. The next section will delve further into local magnetic field anomalies detected from our measurements. A small note- data from AMR and OVR stations in missing in Fig. 7, as this (i.e. Feb 19th) was the only day a GMD event occurred since the network first went online in Jan 2020. Coincidentally on this day, these two stations were offline for maintenance. The maintenance was partly driven by some inconsistent data detected from these two stations, which is reflected in the correlation results of AMR and OVR from two weeks before the event. The TAMUMN has tools built in to detect bad or suspicious data and raise warnings etc.

B. Magnetic Field Time Series

The goal here is to give the readers an idea of what the magnetic field looks like on a usual day versus during a GMD event. The variation in the x-component of the magnetic field at four stations is shown for a 6-hr window on a non-event day in Fig. 8, and the on the day of the G1 event in Fig. 9.

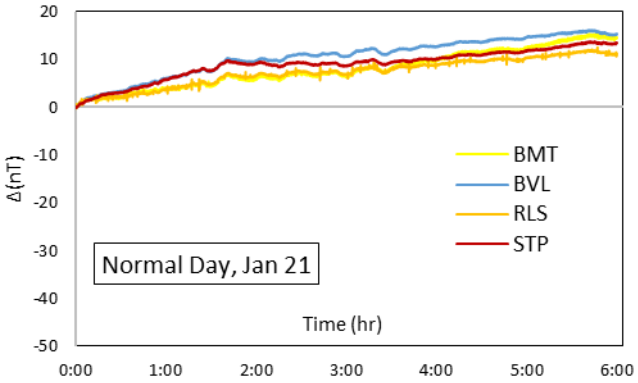

Fig. 8. Change in the magnetic field x-component on a normal day

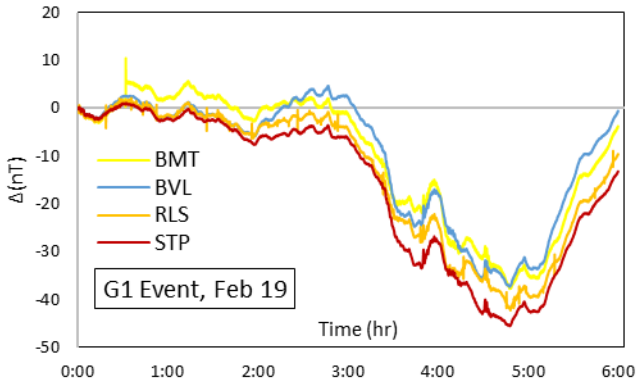

Fig. 9. Change in the magnetic field x-component on a GMD Event Day

This change (measured in nT) is calculated by subtracting from the entire window, the value at the first time point in order to start from zero. The key differences between the data on the two days are in the extent and the rate of change of the magnetic field, with the G1 event day showing more pronounced characteristics.

C. Real-time Visualization

The data from each station is streamed online in CSV format, which is queried every second. A dashboard is developed using the Open Source tool Grafana [31] which receives magnetic field data as an input, with values updated every second to display on a time-varying graph. Small to large time-frames (looking back secs. to days) can be chosen using the interface, to view the three components in real-time. This dashboard is part of an ongoing effort of enabling interactive data access to the industry and research community. The idea is to make this data available for both offline (e.g. CSV file download for post-event analysis) and online (e.g. real-time monitoring) applications.

Fig. 10 visualizes multiple data streams (AMR, BMT, BVL, RLS, and STP). Note here the order of magnitude difference between the y-component (bottom plot) of the BMT data (yellow curve) and RLS (orange curve) compared to the AMR, BVL, and STP data. Such behavior is not seen in the x and z components. The variation in the y-component reflects the difference in local declination, or the difference between geomagnetic and geographic north. Such drastic differences across the sites could be due to, 1) local magnetic field anomalies that rotate the field orientation and/or 2) errors in instrument alignment. One way to verify this is to compare the measurements with the World Magnetic Model (WMM) [32], which estimates the geomagnetic field at a location. The BMT and RLS data agreed well with the WMM results in terms of the order of magnitude of the y-component, potentially ruling out instrument misalignment and alluding to the possibility of a local anomaly and field rotation. Work is ongoing to confirm this; yet this initial observation demonstrates a key application of the TAMUMN, i.e. model validation made possible by this unique array of closely spaced magnetometers.

D. Detection of Geomagnetic Pulsations

Apart from GMDs caused by CMEs, Earth's magnetosphere can be disturbed by phenomena such as sudden storm commencements (SSCs), geomagnetic pulsations, and auroral substorms. Geomagnetic continuous pulsations (Pc) are caused by the interaction between the solar wind and the magnetosphere. They cover the frequency range of about 2 mHz to 5 Hz. Pc waves are classified into five types depending on their period, with Pc1 having a period of 0.2-5 sec, and the quasi-sinusoidal Pc5 with a 150-600 sec period.

On 23rd June, 2020, magnetic field oscillations with a 10-min period were observed for 30 minutes at magnetometers around the world (Hawaii and Boulder to China, Arctic Circle to Antarctica) at the same time [33], including the TAMUMN. Fig. 11 shows the change in the magnetic field x-component for three TAMUMN stations namely BMT, BVL, and STP and one USGS station (BOU). The approximately 10-min period can be seen between 6:35 and 6:55 AM, along with the slightly sinusoidal nature of the variation. Ground currents with the same period were also detected at some locations at this time. However, there was no major change in solar wind speed or other factors to explain this disturbance. This is because they were caused by Pc5 pulsations, which are generated from a resonance condition. The solar wind flow triggers surface waves along the flanks of the magnetopause which can generate standing oscillations in the magnetosphere that penetrate and dissipate towards the Earth [34]. On the ground, the pulsation amplitude can range from tenths to hundreds of nT, and generally increases with the period and magnetic latitude.

Pc5 waves can exist during both active or quiet solar times. However, they stand out during quiet times as was the case in June 2020, as opposed to getting masked by the more intense GMDs. It was noted as a global magnetic anomaly, during

Fig. 10. Real-time magnetometer data looking back over a 20-hr period from June 10th, 4:00 PM on a normal day at multiple stations

what was being touted as possibly the deepest solar minimum in a century [33]. From a power grid GIC perspective, Pc5 waves can be important since GIC activity in subauroral latitudes depends on the storm phase and on the interplanetary drivers, such as CMEs and corotating interacting regions (CIRs) [35]. GIC amplitudes are relatively small during CIRs as compared to CMEs; however, Pc5 pulsation activity during CIRs can lead to long-lasting GICs as observed and concluded from past events. Magnetometers such as the TAMUMN open up opportunities to better understand such unique phenomena. This can then help develop better relationships between the solar wind and other geophysical drivers, and GICs flowing in the ground and the power grid.

IV. Summary and Future Work

GMDs can significantly impact the power grid, however, there are many uncertainties in their modeling. GMD-related measurements can help improve modeling, analysis, situational awareness and consequently the preparedness against such events. Hence, this paper demonstrates a magnetic field monitoring system leveraging the newly installed TAMUMN. The active network streams real-time magnetometer data which is visualized and analyzed. The data is well-correlated among its individual stations, as well as with data from existing magnetic observatories in the US. Work on further understanding the local anomalies and differences will continue with more data collection and as more GMD events are encountered. A key task is to identify any unique insights such a closely spaced array of magnetometers at lower latitudes can offer, in terms of capturing higher frequency data or understanding local field intensifications.

Another important direction is to combine this data with actual GIC measurements from nearby transformers recorded during GMD events. This will be useful for estimating the ground response, which is a major source of uncertainty in this region at present, and hence improve modeling and analysis of the GMD threat. The data is also being used to develop applications such as GIC estimation to supplement GIC monitor data, and real-time visualization and control applications for research on improving power system operations under a GMD. A key ongoing task is also to make the data system compatible with or migrate to a more industry standard tool such as the OSIsoft PI system, towards easier access to this data for utilities/industry/researchers.

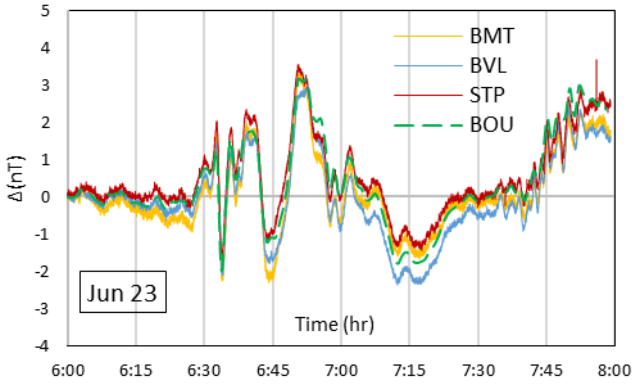

Fig. 11. Change in the magnetic field x-component on June 23, 2020 (day of Pc5 event)

References

[1] V. D. Albertson, J. G. Kappenman, N. Mohan, and G. A. Skarbakka, "Load-Flow Studies in the Presence of Geomagnetically-Induced Currents," *IEEE Transactions on Power Apparatus and Systems*, vol. PAS-100, no. 2, pp. 594–607, 1981.

[2] V. D. Albertson, J. M. Thorson, R. E. Clayton, and S. C. Tripathy, "Solar-Induced-Currents in Power Systems: Cause and Effects," *IEEE Transactions on Power Apparatus and Systems*, vol. PAS-92, no. 2, pp. 471–477, March 1973.

[3] "IEEE Draft Guide for Establishing Power Transformer Capability while under Geomagnetic Disturbances," *IEEE PC57.163/D2.5, July 2015*, pp. 1–55, 2015.

[4] "High-Impact, Low-Frequency Event Risk to the North American Bulk Power System," North American Electric Reliability Corporation (NERC), Tech. Rep., June 2010.

[5] "Effects of geomagnetic disturbances on the bulk power system," North American Electric Reliability Corporation (NERC), Tech. Rep., Feb 2012.

[6] T. J. Overbye, K. S. Shetye, T. R. Hutchins, Q. Qiu, and J. D. Weber, "Power grid sensitivity analysis of geomagnetically induced currents," *IEEE Transactions on Power Systems*, vol. 28, no. 4, pp. 4821–4828, Nov 2013.

[7] V. D. Albertson, J. M. Thorson, and S. A. Miske, "The effects of geomagnetic storms on electrical power systems," *IEEE Transactions on Power Apparatus and Systems*, vol. PAS-93, no. 4, pp. 1031–1044, 1974.

[8] V. Albertson, B. Bozoki, W. Feero, J. Kappenman, E. Larsen, D. Nordell, J. Ponder, F. Prabhakara, K. Thompson, and R. Walling, "Geomagnetic disturbance effects on power systems," *IEEE Transactions on Power Delivery*, vol. 8, no. 3, pp. 1206–1216, 1993.

[9] "Geomagnetic disturbance effects on power systems," *IEEE Transactions on Power Delivery*, vol. 8, no. 3, pp. 1206–1216, 1993.

[10] J. J. Love and C. A. Finn, "The USGS Geomagnetism Program and its role in space weather monitoring," *Space Weather*, vol. 9, no. 7, pp. 1–5, 2011.

[11] D. Kerridge, "INTERMAGNET: Worldwide near-real-time geomagnetic observatory data," in *Proceedings of the workshop on space weather, ESTEC*, vol. 34, 2001.

[12] J. J. Love and A. Chulliat, "The IMAGE Magnetometer Network," *EOS, Transactions, American Geophysical Union*, vol. 94, no. 42, pp. 373–374, Oct 2013.

[13] J. W. Gjerloev, "The SuperMAG data processing technique," *Journal of Geophysical Research: Space Physics*, vol. 117, no. A9, 2012.

[14] A. W. P. Thomson, "Geomagnetic observatories: monitoring the earth's magnetic and space weather environment," *Weather*, vol. 69, no. 9, pp. 234–237, 2014.

[15] H. Lühr, "The IMAGE Magnetometer Network," *NOAA National Centers for Environmental Information*, 1994. [Online]. Available: https://space.fmi.fi/image

[16] "USGS Geomagnetic Observatories." [Online]. Available: https://www.usgs.gov/natural-hazards/geomagnetism/science/observatories?qt-science_center_objects=0#qt-science_center_objects

[17] M. Kazerooni, H. Zhu, and T. J. Overbye, "Use of sparse magnetometer measurements for geomagnetically induced current model validation," in *2015 North American Power Symposium (NAPS)*, 2015, pp. 1–6.

[18] "Improving Conductivity Models for Geomagnetically Induced Current Estimation," Electric Power Research Institute (EPRI), Tech. Rep., March 2020.

[19] H. Zhu, "Power network flow blocking for mitigating the effects of geomagnetically induced currents," in *2014 IEEE Global Conference on Signal and Information Processing (GlobalSIP)*, 2014, pp. 862–66.

[20] "TPL-007-2 Transmission System Planned Performance for Geomagnetic Disturbance Events," North American Electric Reliability Corporation (NERC), Tech. Rep., Oct 2017.

[21] Xie YanQiong, Zhang Jun, and Han XianHua, "Ensemble forecasting model for geomagnetic disturbance," in *Proceedings of 2011 International Conference on Electronics and Optoelectronics*, vol. 1, 2011, pp. V1–335–V1–338.

[22] "Guide for Magnetic for Repeat Station Surveys," International Association of Aeronomy and Geomagnetism (IAGA), Tech. Rep., 1996.

[23] "Space Hazard Monitor for Real time GMD Assessment." [Online]. Available: http://www.gicmagnetics.com/SHM1.pdf
[24] "Mag-13 Three-Axis Magnetic Field Sensors," *Bartington Instruments*. [Online]. Available: https://www.bartington.com/wp-content/uploads/pdfs/datasheets/Mag-13_DS3143.pdf
[25] "IAGA2002 Data Exchange Format," 2015. [Online]. Available: https://www.ngdc.noaa.gov/IAGA/vdat/IAGA2002/iaga2002format.html
[26] "The JSON Data Interchange Syntax," *Standard ECMA-404*, 2017.
[27] C. Klauber, K. Shetye, T. Overbye, and K. Davis, "A GIC Estimator for Electric Grid Monitoring During Geomagnetic Disturbances," *IEEE Transactions on Power Systems*, vol. 35, no. 6, pp. 4847–4855, Nov 2020.
[28] G. Juvekar, C. Klauber, , K. Davis, T. Overbye, and K. Shetye, "A GIC-Inclusive State Estimator for Power System Awareness during Geomagnetic Disturbance Even," *IEEE Transactions on Power Systems*, pp. 1–1, 2020.
[29] "Magnetometer Coordinate Systems." [Online]. Available: http://www.nerc-bas.ac.uk/public/uasd/instrums/magnet/hdz.html
[30] "INTERMAGNET Data," 2020. [Online]. Available: https://www.intermagnet.org/data-donnee/download-eng.php#
[31] "Grafana Data," 2020. [Online]. Available: https://grafana.com/docs/grafana/latest/features/datasources/influxdb/
[32] "World Magnetic Model 2020," *NOAA National Centers for Environmental Information*, May 2020. [Online]. Available: https://www.ngdc.noaa.gov/geomag/WMM/
[33] "Space Weather," June 23, 2020. [Online]. Available: spaceweather.com
[34] "Magnetic Pulsations," 2020. [Online]. Available: http://roma2.rm.ingv.it/en/themes/22/magnetic_pulsations
[35] R. Kataoka and A. Pulkkinen, "Geomagnetically induced currents during intense storms driven by coronal mass ejections and corotating interacting regions," *J. Geophys. Res.*, vol. 113, no. A03S12, pp. 1–8, 2008.